

naturally occurring functional groups, and whose binding properties are suitable for a wide variety of applications.²⁵ In addition, the functionalized protein should be easy to prepare with minimal purification.

A technique initially described by Gauchet et al.²⁶ fulfills these criteria for soluble proteins by introducing a bioorthogonal azide or alkyne moiety that can be coupled to a complementary alkyne or azide on the surface by a Huisgen [3 + 2] cycloaddition reaction. In this approach, a farnesyl diphosphate derivative bearing an ω -alkyne or ω -azide moiety is attached to the sulfhydryl moiety of the cysteine residue in a C-terminal 'CaaX' recognition motif by protein farnesyltransferase (PFTase).²⁷ The CaaX tetrapeptide, where "C" is cysteine, "a" is a small hydrophobic amino acid, and "X" is alanine, serine, methionine, or asparagine,²⁸ can easily be appended by genetic engineering. Gauchet et al. demonstrated this immobilization strategy on glass surfaces for the Cu⁺ catalyzed Huisgen [3 + 2] cycloaddition and Staudinger reactions.²⁶ This paper reports the adaptation of this approach for regioselective attachment of proteins to self-assembled monolayers on gold surfaces, which can be used in a variety of analyses, including surface plasmon resonance (SPR) and electrochemical applications.²⁹

EXPERIMENTAL PROCEDURE

Preparation of ω -Azide SAMs. ω -Azide alkanethiol SAMs were prepared on gold slides by swirling the slides at 100 rpm in ethanol containing 2 mM (total concentration) thiols **1** and **2** (see Scheme S1) for 44–48 h at rt. The coated slides were swirled three times, 15 min each, with ethanol, and dried with a gentle stream of N₂.

ω -Azide dithiocarbamate SAMs were prepared on gold slides by swirling the slides at 100 rpm in ethanol containing 2 mM (total concentration) amines^{26,30} **3** and **4** (see Scheme 2) and 2 mM carbon disulfide for 44–48 h at rt. The coated slides were swirled three times, 15 min each, with ethanol and dried with a gentle stream of N₂.

Covalent Attachment of Modified Proteins to SAMs on Gold Slides. A silicon mat was attached to a SAM-coated gold slide. A solution of GFP-CVIA, GST-CVIA, or proG-CVIA modified at the C-terminal cysteine with farnesyl (GFP-CVIAf and GST-CVIAf) or propargylfarnesyl (GFP-CVIApf, GST-CVIApf, and proG-CVIApf) moieties was added to individual wells, followed by 0.5 mM CuSO₄, 50 μ M TBTA, and 0.5 mM TCEP (final volume 10 μ L). The slide was swirled at 80 rpm for 4 h at rt. The mat was removed, and the slide was swirled overnight in PBST, pH 7.2, containing 1% BSA and 0.1% Tween 20 at 4 °C. The slide was washed twice with PBST buffer for 30 min. The slide was stored in PBS (pH 7.4) at 4 °C before use.

Antibody Conjugation. Slides in a nitrogen-filled chamber were swirled at 100 rpm with 4 mL of an antibody solution (Alexa Fluor 488-conjugated antiGFP, Alexa Fluor 488-conjugated antiGST, DyLight 680-conjugated anti-GFP, or Alexa Fluor 680-labeled goat anti-rabbit IgG, 0.5–2 μ g/mL) in PBS buffer at 4 °C for 18 h or at rt for 2 h. The slides were washed with PBST buffer 3 times for 30 min and scanned with a Typhoon 8600 Variable Mode Imager.

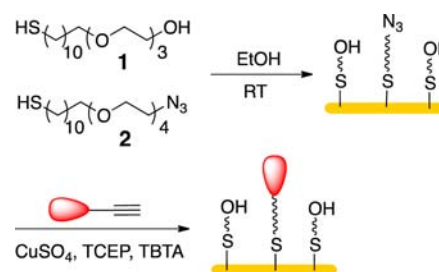
Preparation of DTC-SAM Gold Slides Coated with ProG-CVIApf. Gold slides modified with DTC-SAMs were prepared as described above. Whole surface-coated slides with proG-CVIApf were prepared according a method previously described.³⁰ A slide was covered with an mSeries LifterSlip

coverslip, and 60 μ L of a solution containing 0.5 mM CuSO₄, 50 μ M TBTA, 0.5 mM TCEP, and 50 μ M proG-CVIApf was inserted at the edge of the coverslip. The slide was shaken at 70 rpm for 4 h at rt. After three 1 h washes with PBST buffer, the slide was dried under N₂ and a silicon mat was attached. Ten microliter portions of a series of concentrations of anti-GST rabbit IgG in PBS buffer were added to the wells and the slide was incubated for 2 h at rt. The silicon mat was removed, the slide was washed with PBST buffer three times for 1 h at rt, and the slide was visualized.

RESULTS AND DISCUSSION

PEG-Alkane Spacers and Linkers. PEG-alkane derivatives were prepared with azide groups attached to the PEG end of the molecules and hydroxyl (spacer), thiol (linker), or amine (linker) groups on the hydrocarbon end (see Scheme 1 for

Scheme 1. Preparation of Thiol-SAMs on Gold Surfaces and Immobilization of GST-CVIApf by a Huisgen [3 + 2] Cycloaddition



structures). Thiols **1** (spacer) and **2** (linker) were prepared by the general protocol reported by Pale-Grosdemange et al. (Scheme S1).³¹ Spacer **1** has a hydrophobic undecamethylene chain at the thiol end and a triethylene glycol chain at the hydroxyl terminus. The thiol end of linker **2** is similar, while the azide end of the molecule contains a tetraethylene glycol unit. Amine **3** (spacer) has a hexamethylene unit at the amino end and a triethylene glycol unit at the hydroxyl terminus. Amine **4** (linker) has a hexamethylene unit (amine end) attached to a PEG₈ azide (azide end) through amide linkages to a diglycolic acid spacer.^{26,30}

Preparation of SAMs on Gold Slides and Modified Proteins. SAMs were prepared from ethanol solutions of a mixture of the thiol spacer and linker (thiol SAMs) or a mixture of amine spacer, amine linker, and carbon disulfide for dithiocarbamate (DTC) SAMs. The gold slides were imaged before and after SAM formation. N-terminal His₆-tagged GFP-CVIA and GST-CVIA were expressed and purified as previously described.^{26,29} Incubation of the proteins with FPP (control) or ω -propargylFPP (Figure 1) with PFTase as described by Gauchet et al. gives GFP-CVIAf, GFP-CVIApf, GST-CVIAf, and GST-CVIApf, respectively.²⁶ The modifications were confirmed by ESI MS.³⁰ Modified GFP retained its native fluorescence properties, and modified GST retained its catalytic activity.²⁷ The regio- and chemoselective immobilization of GFP-CVIApf and GST-CVIApf on SAM-coated gold

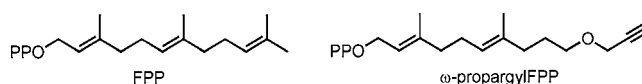


Figure 1. FPP and ω -propargylFPP.

slides was carried out as described by Seo et al. for silica surfaces.³⁰

Covalent Immobilization on Thiol SAMs. The thiol SAM technique has been widely used to attach biological molecules, including antibodies and enzymes, to gold surfaces.^{6,7} Regioselective covalent immobilization of proteins on SAMs can be accomplished without denaturation, resulting in an increased binding capacity and sufficient exposure of functional domains. The alkanethiol assembly on gold was used for site-specific immobilization of GFP-CVIApf and GST-CVIApf shown in Scheme 1. Part A of Figure 2 shows images of

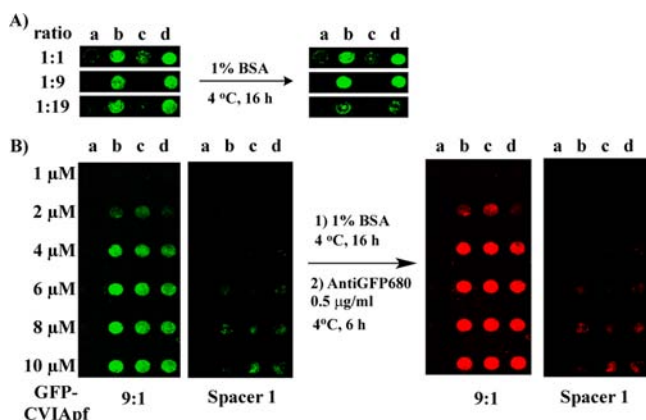


Figure 2. Visualization of GFP immobilized on spacer 1/linker 2 thiol-SAMs. (A) Immobilization of 5 μM GFP-CVIApf: (a) PBS; (b) with 1 mM CuSO_4 , 1 mM TCEP, 100 μM TBTA; (c) with 1 mM CuSO_4 ; (d) with 1 mM CuSO_4 and 1 mM TCEP. (B) Immobilization of various concentrations of GFP-CVIApf: (a) PBS without protein; (b) with protein, 0.5 mM CuSO_4 , 0.5 mM TCEP; (c) and (d) with protein, 0.5 mM CuSO_4 , 0.5 mM TCEP, 50 μM TBTA. First slide in each set was coated with a 9:1 molar ratio of spacer 1 and linker 2; second slide was coated with spacer 1. Fluorescence intensity was measured at $\lambda_{\text{Ex}} = 532/\lambda_{\text{Em}} = 526$ nm for the detection of GFP and at $\lambda_{\text{Ex}} = 633/\lambda_{\text{Em}} = 670$ nm for antiGFP680.

wells where GFP-CVIApf in PBS buffer was attached to SAMs containing different ratios of spacer 1 and linker 2. Lane a is a copper-free control; lane b has CuSO_4 , TCEP, and TBTA; lane c contains CuSO_4 ; and lane d has CuSO_4 and TCEP. A 9:1 ratio of 1:2 gave optimal performance (i.e., high sensitivity and low background). Immobilizations with higher concentrations of GFP-CVIApf (20 and 80 μM) on thio-SAMs containing different ratios of spacer 1 and linker 2 were examined, confirming that a 9:1 ratio of 1:2 was optimal (Figure S1). As expected, GFP-CVIApf was not efficiently immobilized in wells without Cu(I) or with CuSO_4 and no TCEP reductant, although a small amount of immobilization, presumably nonspecific, was observed in wells containing CuSO_4 , apparently promoted by the presence of Cu(II) . This amount increases in the wells containing CuSO_4 and TCEP, a phenomenon previously reported by Speers and Cravatt.³² Under our conditions, Cu^{2+} does not promote significant nonspecific binding of GFP-CVIApf.

Part B of Figure 2 shows fluorescence intensities for pairs of slides with SAMs consisting of 9:1/spacer 1:linker 2 (left) or only spacer (right). Individual wells contained 1–10 μM GFP-CVIApf and CuSO_4 /TCEP/TBTA in PBS buffer. The slides coated with spacer 1:linker 2 (9:1) showed a concentration-dependent increase in fluorescence intensity for GFP. Detection of GFP fluorescence established that the native

protein remained folded after immobilization. As expected, no fluorescence was observed in control wells without protein. Very weak spots of fluorescence for GFP-CVIApf detected on the spacer-only slides indicated that a small amount of the protein remained on the SAM after washing. Similar patterns were observed after an additional 16 h wash when the slides were imaged at higher sensitivity with fluorescent antiGFP680. Significant levels of fluorescence were observed in those wells treated with 4–10 μM of GFP-CVIApf, indicating that a ~ 5 μM concentration of the alkyne-modified protein was sufficient for detection.

In a second set of experiments (Figure 3), fluorescence intensity was measured in wells of slides coated with spacer

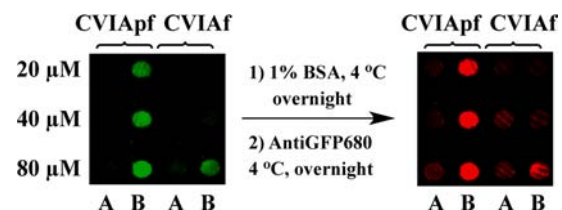


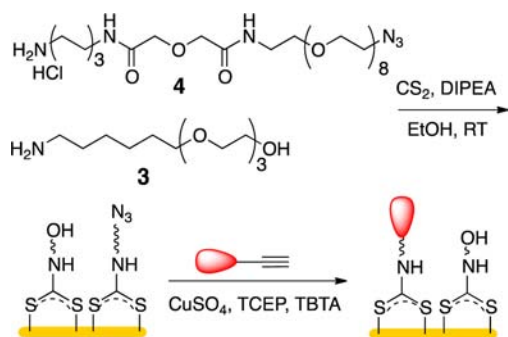
Figure 3. Visualization of GFP-CVIApf and GFP-CVIAf on 1:9 spacer 1:linker 2 thiol-SAMs. Lane A: 50 μM CuSO_4 , 50 μM TCEP, 50 μM TBTA. Lane B: 0.5 mM CuSO_4 , 0.5 mM TCEP, 50 μM TBTA. Fluorescence intensity was measured at $\lambda_{\text{Ex}} = 532/\lambda_{\text{Em}} = 526$ nm for the detection of GFP and at $\lambda_{\text{Ex}} = 633/\lambda_{\text{Em}} = 670$ nm for antiGFP680.

1:linker 2 (9:1) containing varying concentrations of GFP-CVIApf or GFP-CVIAf. Lane A contained 50 μM CuSO_4 , 50 μM TCEP, and 50 μM TBTA, while lane B contained 500 μM CuSO_4 , 500 μM TCEP, and 50 μM TBTA. The wells in lane A for GFP-CVIApf did not fluoresce, while those in lane B gave a concentration-dependent pattern with strong fluorescent intensities at the higher concentrations, as expected for attachment of the protein to linker 2 (Figure 2S). The difference between lanes A and B indicated that 50 μM concentrations of CuSO_4 and TCEP in the copper catalyst mixture were not sufficient to efficiently couple the protein with the SAM linker. For GFP-CVIAf, which is not a substrate for the Huisgen [3 + 2] cycloaddition, no signals were observed in lane A and a weak signal was detected in lane B for the well containing 80 μM protein. The fluorescence observed in lane B for 80 μM GFP-CVIAf suggests a low level of copper-catalyzed attachment of the protein to the SAM. The intensity of the signals increased substantially when the slides were incubated with strongly fluorescent antiGFP680.

Protein Immobilization on DTC-SAMs. The most commonly used procedure for preparing SAMs on gold surfaces is by chemisorption of thiols. However, surface-bound thiols chemisorbed by a single sulfur–gold bond can leach from the gold surfaces, and care must be taken during synthesis and storage of thiols to prevent oxidation. Recently, Zhao and co-workers reported formation of SAMs with dithiocarbamate (DTC) linkages to gold surfaces by treatment with a mixture of an amine and carbon disulfide (CS_2).¹⁵ The enhanced stability of the DTC-SAMs in acidic and basic conditions was attributed to superior chemisorption properties due to the formation of two sulfur–gold bonds.^{33,34}

We prepared DTC-SAMs by shaking gold-coated slides in an ethanol solution of CS_2 and primary amines, spacer 3 and linker 4, which we previously attached to silica surfaces through urea linkages³⁰ (Scheme 2). Unlike thiol-SAMs, there was no significant difference in the fluorescence intensities of GFP-

Scheme 2. Preparation of DTC-SAMs on Gold Surfaces and Immobilization of GST-CVIApf by a Huisgen Cycloaddition



CVIApf on SAMs prepared with different molar ratios of spacer 3 and linker 4 (Figure 4A) when measured directly or after

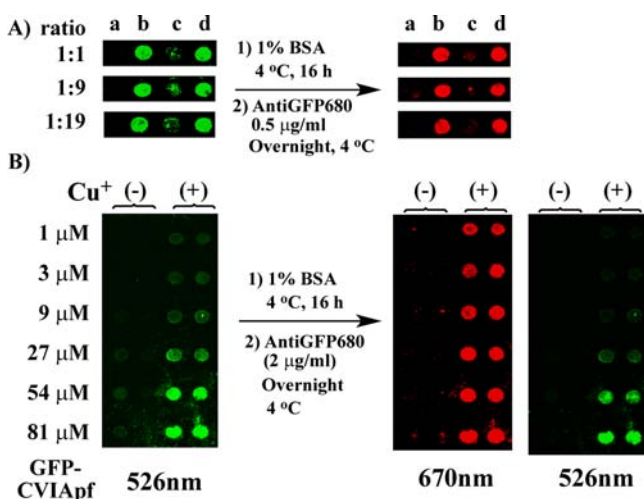


Figure 4. Visualization of GFP-CVIApf immobilized on different molar ratios of spacer 3/linker 4 DTC-SAMs. (A) 5 μ M GFP-CVIApf: (a) PBS; (b) 1 mM CuSO_4 , 1 mM TCEP, 100 μ M TBTA in PBS; (c) 1 mM CuSO_4 in PBS; (d) 1 mM CuSO_4 and 1 mM TCEP in PBS. (B) Varied concentrations of GFP-CVIApf; 0.5 mM CuSO_4 (+) and without CuSO_4 (–), 0.5 mM TCEP and 50 μ M TBTA in PBS; slide was coated with a 9:1 molar ratio of spacer 3 and linker 4. Fluorescence intensity was measured at $\lambda_{\text{Ex}} = 532/\lambda_{\text{Em}} = 526$ nm for the detection of GFP and at $\lambda_{\text{Ex}} = 633/\lambda_{\text{Em}} = 670$ nm for antiGFP680.

incubation with fluorescent antiGFP680. As observed for the thiol SAMs, wells without Cu(I) did not fluoresce (lane a, Figure 4A); those containing CuSO_4 were weakly fluorescent, while those containing CuSO_4 and a mixture of TCEP and TBTA or TCEP alone gave strong signals. These trends were observed for direct visualization of GFP or indirect detection with fluorescent antiGFP680.

GFP-CVIApf (1 to 81 μ M) was immobilized using 0.5 mM CuSO_4 , 0.5 mM, and 50 μ M TBTA. A concentration-dependent pattern of emission at 526 nm for the GFP fluorophore was observed in the wells treated with 1–9 μ M GFP-CVIApf (left slide, Figure 4B). The slide was then washed PBST buffer containing 1% BSA for 16 h. Visualization of GFP fluorescence, monitored at 526 nm following excitation at 532 nm, gave a similar pattern, while visualization of the antiGFP680 fluorophore at 670 nm (excitation at 633 nm) gave intense spots at all concentrations of immobilized GFP-CVIApf.

The experiments described in Figure 3 were repeated for gold slides coated with DTC-SAMs formed from spacer 3 and linker 4 (9:1) with similar results (Figure 5). GFP fluorescence

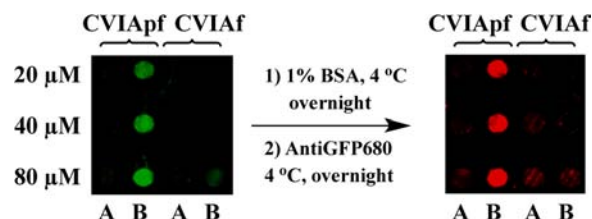


Figure 5. Visualization of GFP-CVIApf and GFP-CVIAf on 1:9 spacer 3:linker 4 DTC-SAMs. (A) 50 μ M CuSO_4 , 50 μ M TCEP, 50 μ M TBTA. (B) 0.5 mM CuSO_4 , 0.5 mM TCEP, 50 μ M TBTA. The slide was incubated with AntiGFP680 (2 μ g/mL). Fluorescence intensity was measured at $\lambda_{\text{Ex}} = 532/\lambda_{\text{Em}} = 526$ nm for the detection of GFP and at $\lambda_{\text{Ex}} = 633/\lambda_{\text{Em}} = 670$ nm for antiGFP680.

was observed in wells treated with 500 μ M CuSO_4 , 500 μ M TCEP, 50 μ M TBTA, and 20–80 μ M GFP-CVIApf; and very weak signals were detected in wells treated with 500 μ M CuSO_4 , 500 μ M TCEP, 50 μ M TBTA, or those treated with 500 μ M CuSO_4 , 500 μ M TCEP, 50 μ M TBTA, and 80 μ M GFP-CVIAf. The intensity of the spots increased when visualized with antiGFP680.

The selectivity for detection of immobilized proteins by fluorescent antibodies was determined with a gold slide coated with DTC SAMs. GST-CVIApf and GFP-CVIApf were immobilized in wells on the top and bottom halves of the slide, respectively, washed and imaged. Fluorescence was observed for the GFP fluorophore (Figure 6). The slide was washed again and incubated with a mixture of antiGST488 and antiGFP680. When the slide was imaged, fluorescence was detected at 526 nm (excitation 532) nm for wells containing GST-CVIApf and at 670 nm (excitation at 633 nm) for wells containing GFP-CVIApf. When the slide was imaged at 532/526 nm, fluorescence was detected in wells immobilized with GFP-CVIApf along with wells containing antiGST488. However, fluorescence intensity of GFP-CVIApf at 532/526 nm is weak compared to that of antiGST488, and only antiGST488 was visualized when their fluorescence intensities were measured together.

Quantitation of Immobilized proG-CVIApf on Thiol and DTC-SAM Coated Slides. Different concentrations of proG-CVIApf were spotted into wells of a matted slide coated with thiol- and DTC-SAMs. The mat was removed before the slide was washed and incubated with Alexa680 goat anti-rabbit IgG. Plots of fluorescence intensity as a function of proG-CVIApf concentration showed that the increase in fluorescence reached a plateau when 10 μ L of a ~ 1.6 μ M solution of proG-CVIApf (5.1 pmol/ mm^2) was used for immobilization to the thiol SAM (Figures 7 and S4). For the DTC-SAM surface, the plateau was reached when 10 μ L of a ~ 16 μ M proG-CVIApf solution (51 pmol/ mm^2) was applied.

A surface coated DTC-proG-CVIApf slide was prepared by treatment with 30 μ L of a solution containing 100 μ M proG-CVIApf (2.3 pmol/ mm^2) and 30 μ L of Cu(I) buffer. A silicon mat was attached and 10 μ L samples of a series of concentrations of Alexa488 anti-GST rabbit IgG (MW ~ 150 K) were spotted into the wells. A plot of fluorescence intensity versus concentration indicates that 10 μ L of a 20 μ g/

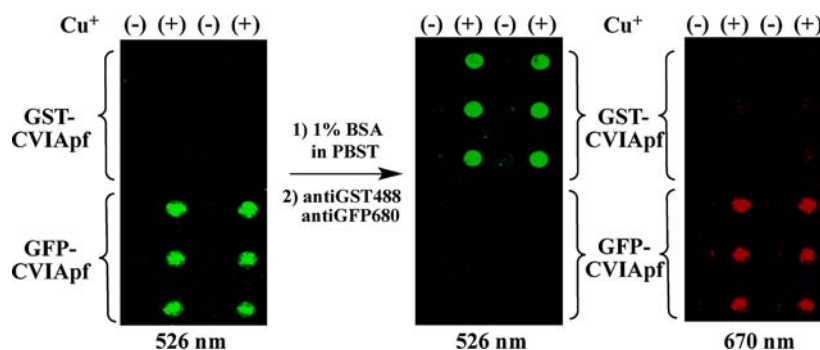


Figure 6. Selective detection of GST and GFP with fluorescent antibodies. GST-CVIApf and GFP-CVIApf (80 μ M) were immobilized on the same slide (1:9 spacer 3:linker 4 DTC-SAMs), and then incubated with a mixture of antiGST488 (2 μ g/mL) and antiGFP680 (2 μ g/mL). Well treated with (+) and without (–) Cu^+ . Fluorescence intensity was measured at $\lambda_{\text{Ex}} = 532/\lambda_{\text{Em}} = 526$ nm for detection of antiGST and at $\lambda_{\text{Ex}} = 633/\lambda_{\text{Em}} = 670$ nm for antiGFP.

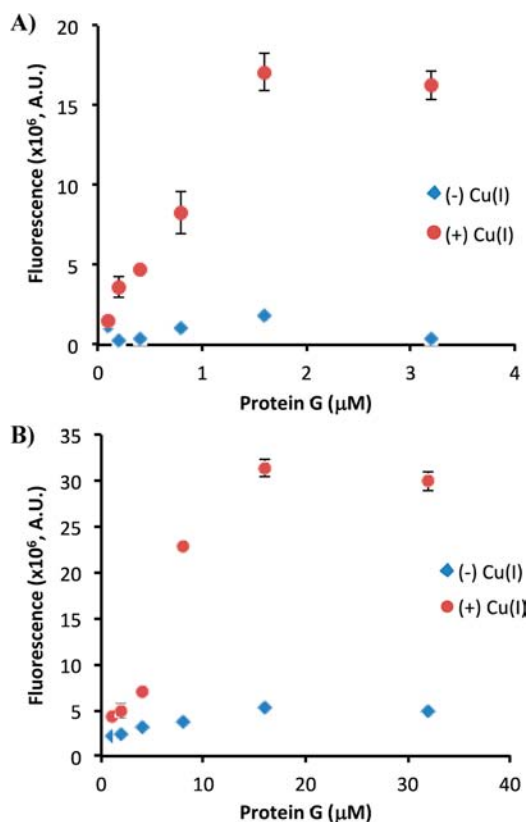


Figure 7. Plots of fluorescence intensities vs varied concentrations of protein G. ProG-CVIApf was immobilized on 9:1 molar ratio of spacer/linker (A) thiol-SAMs or (B) DTC-SAMs by Cu(I) catalyzed cycloaddition (0.5 mM CuSO_4 , 0.5 mM TCEP, 0.05 mM TBTA). The slides were incubated with Alexa 680 labeled goat anti-rabbit IgG (1 μ g/mL). Well treated with (+) and without (–) Cu^+ . Fluorescence intensity was measured at $\lambda_{\text{Ex}} = 633/\lambda_{\text{Em}} = 670$ nm for the detection.

μ L solution (0.42 pmol/ mm^2) of the antibody saturates the binding sites of immobilized proG-CVIApf (Figures 8 and S5).

Displacement of Immobilized Proteins in Thiol- and DTC-SAMs by β -Mercaptoethanol. The relative ease of displacing immobilized proteins from thiol and DTC SAMs on gold slides was examined with a solution of β -mercaptoethanol (BME) in ethanol. Slides with GFP-CVIApf immobilized on thiol and DTC-SAMs were incubated in a solution of BME in ethanol and imaged with antiGFP680. The intensity of the fluorescent signals of wells on thiol-SAMs decreased by

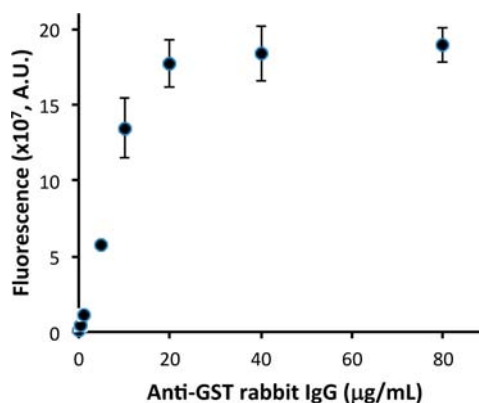


Figure 8. Plot of fluorescence intensity vs varied concentration of anti-GST rabbit IgG. ProG-CVIApf (50 μ M) was immobilized on a slide with 9:1 molar ratio of spacer/linker DTC-SAM by Cu(I) catalyzed cycloaddition (0.5 mM CuSO_4 , 0.5 mM TCEP, 0.05 mM TBTA). A series of 10 μ L samples of different concentrations of anti-GST rabbit IgG (Alexa Fluor 488 conjugate) were spotted in the wells. Fluorescence intensity was measured at $\lambda_{\text{Ex}} = 532/\lambda_{\text{Em}} = 526$ nm.

approximately 94% when incubated in 50 mM BME for 24 h (Figure 9A). A slightly less intense signal was observed after incubation for an additional 24 h in 100 mM BME. After 46 h, the signal had decreased by 99% from its original intensity. In contrast, displacement was much slower for GFP-CVIApf immobilized on DTC SAMs. Under similar conditions, the signal intensity decreased by only 13% after 48 h and 27% after 72 h (Figure 9B). It is evident that the sulfur–gold linkages in DTC-SAMs are substantially more robust than those in thiol SAMs.

CONCLUSION

There are many different approaches for immobilizing proteins to create biochips. The technique described here involving SAM-coated gold surfaces provides a relatively simple general procedure to covalently immobilize proteins regio- and chemoselectively using a bioorthogonal Huisgen [3 + 2] cycloaddition. The immobilized proteins, in this work, GFP, GST, and proG, were immobilized directly from cell-free homogenates chemoselectively and visualized with fluorescent antibodies. While the proteins can be immobilized on either thiol- or DTC-coated gold surfaces, DTC SAMs are more stable and amine-terminated linkers used to construct the SAMs are easier to handle and store than their thiol-terminated

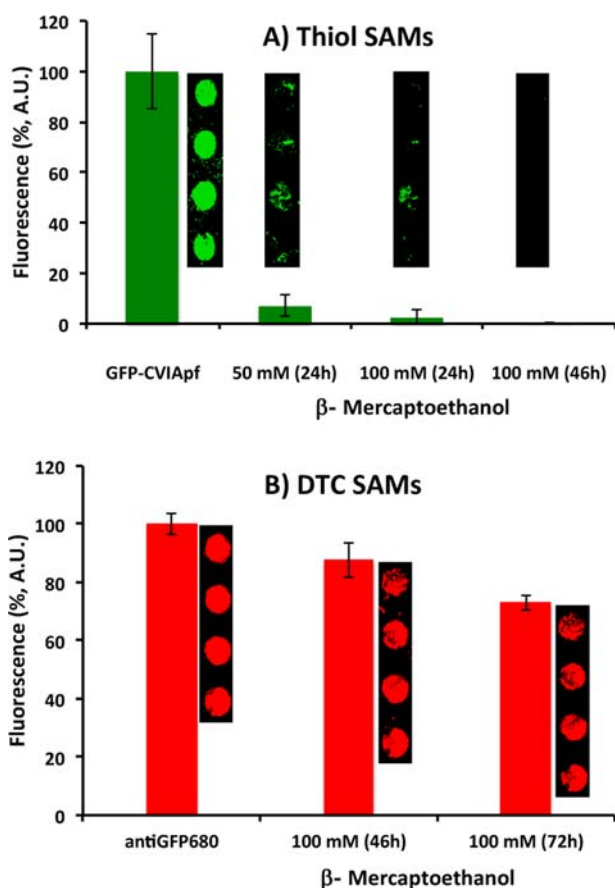


Figure 9. Displacement of SAMs by β -mercaptoethanol: (A) thiol-SAMs; the slide was treated with β -mercaptoethanol after immobilization of GFP (green); (B) DTC-SAMs; the slide was treated with β -mercaptoethanol after incubation with antiGFP680 (red). GFP-CVIApf was immobilized on 9:1 molar ratio of spacer/linker thiol-SAMs or DTC-SAMs by Cu(I) catalyzed cycloaddition (0.5 mM CuSO_4 , 0.5 mM TCEP, 0.05 mM TBTA). Fluorescence intensity was measured at $\lambda_{\text{Ex}} = 532/\lambda_{\text{Em}} = 526$ nm for the detection of GFP and at $\lambda_{\text{Ex}} = 633/\lambda_{\text{Em}} = 670$ nm for antiGFP680.

linkers. When used to immobilize antibody-binding proteins, this technique can be extended to detect a wide variety of molecules.³⁰

■ ASSOCIATED CONTENT

Supporting Information

NMR and MS related to the synthesis are available. This material is available free of charge via the Internet at <http://pubs.acs.org>.

■ AUTHOR INFORMATION

Corresponding Author

*E-mail: poulter@chemistry.utah.edu.

Author Contributions

Seoung-ryoung Choi and Jin-soo Seo contributed equally.

Notes

The authors declare no competing financial interest.

■ ACKNOWLEDGMENTS

This work was supported by NIH grant GM 21328.

■ REFERENCES

- (1) Rusmini, F., Zhong, Z., and Feijen, J. (2007) Protein immobilization strategies for protein biochips. *Biomacromolecules* 8, 1775–1789.
- (2) Lin, P.-C., Weinrich, D., and Waldmann, H. (2010) Protein biochips: oriented surface immobilization of proteins. *Macromol. Chem. Phys.* 211, 136–144.
- (3) Luong, J. H. T., Male, K. B., and Glennon, J. D. (2008) Biosensor technology: Technology push versus market pull. *Biotechnol. Adv.* 26, 492–500.
- (4) Lee, Y.-S., and Mrksich, M. (2002) Protein chips, from concept to practice. *Trends Biotechnol.* 20, S14–S18.
- (5) Braun, R., Sarikaya, M., and Schulten, K. (2002) Genetically engineered gold-binding polypeptides: structure prediction and molecular dynamics. *J. Biomater. Sci., Polym. Ed.* 13, 747–757.
- (6) Abad, J. M., Pita, M., and Fernandez, V. M. (2006) Immobilization of proteins on gold surfaces. *Methods Biotechnol.* 22, 229–238.
- (7) Frascioni, M., Mazzei, F., and Ferri, T. (2010) Protein immobilization at gold-thiol surfaces and potential for biosensing. *Anal. Bioanal. Chem.* 398, 1545–1564.
- (8) Niu, Y., Matos, A. I., Abrantes, L. M., Viana, A. S., and Jin, G. (2012) Antibody oriented immobilization on gold using the reaction between carbon disulfide and amine groups and its application in immunosensing. *Langmuir* 28, 17718–17725.
- (9) Morf, P., Raimondi, F., Nothofer, H.-G., Schnyder, B., Yasuda, A., Wessels, J. M., and Jung, T. A. (2006) Dithiocarbamates: functional and versatile linkers for the formation of self-assembled monolayers. *Langmuir* 22, 658–663.
- (10) Hou, Z., Abbott, N. L., and Stroeve, P. (1998) Electroless gold as a substrate for self-assembled monolayers. *Langmuir* 14, 3287–3297.
- (11) Schoenfish, M. H., and Pemberton, J. E. (1998) Air stability of alkanethiol self-assembled monolayers on silver and gold surfaces. *J. Am. Chem. Soc.* 120, 4502–4513.
- (12) Dasog, M., and Scott, R. W. J. (2007) Understanding the oxidative stability of gold monolayer-protected clusters in the presence of halide ions under ambient conditions. *Langmuir* 23, 3381–3387.
- (13) Schlenoff, J. B., Li, M., and Ly, H. (1995) Stability and self-exchange in alkanethiol monolayers. *J. Am. Chem. Soc.* 117, 12528–36.
- (14) Ryan, D., Parviz, B. A., Linder, V., Semetey, V., Sia, S. K., Su, J., Mrksich, M., and Whitesides, G. M. (2004) Patterning multiple aligned self-assembled monolayers using light. *Langmuir* 20, 9080–9088.
- (15) Zhao, Y., Perez-Segarra, W., Shi, Q., and Wei, A. (2005) Dithiocarbamate assembly on gold. *J. Am. Chem. Soc.* 127, 7328–7329.
- (16) Ulman, A. (1996) Formation and structure of self-assembled monolayers. *Chem. Rev. (Washington, D. C.)* 96, 1533–1554.
- (17) Querner, C., Reiss, P., Bleuse, J., and Pron, A. (2004) Chelating ligands for nanocrystals' surface functionalization. *J. Am. Chem. Soc.* 126, 11574–11582.
- (18) Colorado, R., Jr., Villazana, R. J., and Lee, T. R. (1998) Self-assembled monolayers on gold generated from aliphatic dithiocarboxylic acids. *Langmuir* 14, 6337–6340.
- (19) Zhu, H., Coleman, D. M., Dehen, C. J., Geisler, I. M., Zemlyanov, D., Chmielewski, J., Simpson, G. J., and Wei, A. (2008) Assembly of dithiocarbamate-anchored monolayers on gold surfaces in aqueous solutions. *Langmuir* 24, 8660–8666.
- (20) Eckermann, A. L., Shaw, J. A., and Meade, T. J. (2010) Kinetic dispersion in redox-active dithiocarbamate monolayers. *Langmuir* 26, 2904–2913.
- (21) Dantas de Araujo, A., Palomo, J. M., Cramer, J., Koehn, M., Schroeder, H., Wacker, R., Niemeyer, C., Alexandrov, K., and Waldmann, H. (2006) Diels-Alder ligation and surface immobilization of proteins. *Angew. Chem., Int. Ed.* 45, 296–301.
- (22) Sun, X.-L., Stabler, C. L., Cazalis, C. S., and Chaikof, E. L. (2006) Carbohydrate and protein immobilization onto solid surfaces by sequential Diels-Alder and azide-alkyne cycloadditions. *Bioconjugate Chem.* 17, 52–57.

- (23) Soellner, M. B., Dickson, K. A., Nilsson, B. L., and Raines, R. T. (2003) Site-specific protein immobilization by Staudinger ligation. *J. Am. Chem. Soc.* 125, 11790–11791.
- (24) Cha, T., Guo, A., and Zhu, X.-Y. (2005) Enzymatic activity on a chip: the critical role of protein orientation. *Proteomics* 5, 416–419.
- (25) Wong, L. S., Khan, F., and Micklefield, J. (2009) Selective covalent protein immobilization: strategies and applications. *Chem. Rev. (Washington, DC, U. S.)* 109, 4025–4053.
- (26) Gauchet, C., Labadie, G. R., and Poulter, C. D. (2006) Regio- and chemoselective covalent immobilization of proteins through unnatural amino acids. *J. Am. Chem. Soc.* 128, 9274–9275.
- (27) Viswanathan, R., Labadie, G. R., and Poulter, C. D. (2013) Regioselective covalent immobilization of catalytically active Glutathion S-transferase on glass slides. *Bioconjugate Chem.* 24, 571–577.
- (28) Zhang, F. L., and Casey, P. J. (1996) Protein prenylation: molecular mechanisms and functional consequences. *Annu. Rev. Biochem.* 65, 241–269.
- (29) Cooper, M. A. (2003) Label-free screening of bio-molecular interactions. *Anal. Bioanal. Chem.* 377, 834–842.
- (30) Seo, J.-s., Lee, S., and Poulter, C. D. (2013) Regioselective covalent immobilization of recombinant antibody-binding proteins A, G, and L for construction of antibody arrays. *J. Am. Chem. Soc.* 135, 8973–8980.
- (31) Pale-Grosdemange, C., Simon, E. S., Prime, K. L., and Whitesides, G. M. (1991) Formation of self-assembled monolayers by chemisorption of derivatives of oligo(ethylene glycol) of structure $\text{HS}(\text{CH}_2)_{11}(\text{OCH}_2\text{CH}_2)_m\text{OH}$ on gold. *J. Am. Chem. Soc.* 113, 12–20.
- (32) Speers, A. E., and Cravatt, B. F. (2004) Profiling enzyme activities in vivo using click chemistry methods. *Chem. Biol.* 11, 535–546.
- (33) Coucouvanis, D. (1970) Chemistry of the dithioacid and 1,1-dithiolate complexes. *Prog. Inorg. Chem.* 11, 233–371.
- (34) Arndt, T., Schupp, H., and Schrepp, W. (1989) Self-assembled and Langmuir-Blodgett films of thiocarbaminates: a comparative study. *Thin Solid Films* 178, 319–26.